Structural and luminescence characteristics of SnO_2:Eu and SnO_2:Eu,Sb nanophosphors upon annealing at high temperatures

Valter Kiisk*, Triin Kangur, Madis Paalo, Tanel Tätte, Sven Lange, Siim Pikker, Ilmo Sildos
Institute of Physics, University of Tartu, Riia Str. 142, 51014 Tartu, Estonia

Abstract

The paper explores the structure and luminescence of sol-gel-derived SnO_2:Eu and SnO_2:Eu,Sb nanopowders which may be useful as electrically conductive phosphors. The samples were sintered in air at temperatures reaching up to 1400°C. Raman-, SEM-, EDX- and photoluminescence characterization of the samples was carried out.

High-temperature annealing of SnO_2:Eu leads to a nanoparticulate phosphor with considerable efficiency of host-sensitized Eu^{3+} emission under UV excitation although the emission is slightly quenched at room temperature. While Sb co-dopant immensely improves crystallization at 1400°C, it also impairs luminescence performance. SEM and EDX characterization suggest pronounced segregation of Eu induced by the enhanced crystal growth. Interestingly, Sb-doping seems to activate in the Raman spectrum quite a few SnO_2 vibrations which are normally rather weak or IR active.

PACS: 78.55.Hx, 78.67.Bf, 81.20.Ev, 81.20.Fw
Keywords: ceramics, sol-gel growth, sintering, photoluminescence spectroscopy

1. Introduction

Wide-gap (E_g>3 eV) semiconducting metal oxides like SnO_2 (stannia) or TiO_2 (titania) are technologically attractive as the base materials for transparent conducting media, gas sensors and photocatalysts [1,2]. Moreover, the matrices can be perspective for rare earth (RE) activation owing to the possibility of host-mediated excitation of RE impurities while providing transparency throughout the visible range and reduced thermal quenching of RE emission [3,4]. The host-to-guest energy transfer imposes the potential of carrier-mediated excitation of RE ions as well as the possibility of employing very thin phosphor layers due to the strong absorption of the excitation light by the host. Also, oxides seem to be generally more stable under high load in lighting and display devices compared to e.g. sufides. In particular, electrically conducting phosphors are required for field emission displays [5]. Further promising applications of the materials in photonics arise of their high refractive indices [6]. Trivalent europium appears to be one of the most important RE activators for luminescence applications in visible range as it provides rather pure red or orange hue.

While a number of papers concerning the photoluminescence (PL) of SnO_2:Eu have been published [7–10], consideration of the application potential of the material and possible reasons limiting its luminescence performance is still missing. Hereby, we have carried out a systematic investigation of sol-gel-prepared SnO_2:Eu while also studying the influence of antimony co-dopant, which is one of the main impurities used for improving the electrical conductivity of stannia [1]. Incorporation of co-dopants into RE-doped phosphors may also have additional benefits like sensitizing the RE photoexcitation or improving the solubility of RE ions. While in the present case the antimony co-dopant did not seem to enhance the luminescence properties, it impinged a couple of fairly interesting effects on the structure of the material as revealed by Raman, SEM and EDX data. To the best of our knowledge, the influence of high annealing temperatures (up to 1400°C), the particularities of the Raman spectra of SnO_2:Eu and SnO_2:Sb and the extended excitation spectra of Eu^{3+} in SnO_2 (up to 20 eV) are reported and analyzed for the first time.

2. Samples and experimental

Powders of SnO_2:Eu with 0.5 at% nominal Eu concentration and varied Sb concentration (0, 0.25, 0.5 and 1 at%) was prepared from metal alkoxide precursor by using the sol-gel route [11].

* Corresponding author. Institute of Physics, University of Tartu, Riia Str. 142, 51014 Tartu, Estonia. Tel.: +372-7374613; fax: +372-7383033; e-mail: kiisk@ut.ee

Briefly, 10% water solution in propanol, acidified by 10 drops of concentrated HCl, was added into a solution of neat $Sn(OPr)_4$ in propanol so that water/alkoxide molar ratio was 0.29. For Eu or Sb incorporation, suitable amount of $EuCl_3*xH_2O$ or $SbCl_3$ solution in propanol was added into the alkoxide solution. The mixture was concentrated by using Büschi rotator evaporator. The obtained viscous polymeric substance was left for ageing in air. Powder was formed during a couple of weeks of ageing as a result of the fragmentation of the precursor as the capillary forces overcome the strength of the gel. The powder was grinded in mortar and parts of it were annealed in air for 1 hour at temperatures ranging from 600 to 1400°C.

The as-prepared SnO_2:Eu powder had a beige-like color which turned to a greenish yellow tint after heat treatment at 600°C. The hue gradually faded until the material becomes pure white after annealing at 1200°C. Antimony co-dopant adds a slight bluish hue to the material.

Photoluminescence emission spectra were obtained by exciting the sample with a pulsed tunable OPO light source from Expla Ltd (pulse duration 3 ns, pulse energy ~20 μJ, repetition rate 20 Hz). The spectra were recorded by using a spectrograph (Andor SR-303i, spectral resolution 1 nm) equipped with an image-intensified charge coupled device (Andor DH-501). Luminescence decay kinetics was recorded by employing a Hamamatsu photomultiplier tube (H8259-01) operating in photon counting mode (the spectral width of the emission spectrograph was 20 nm). For measurement of excitation spectra, a synchrotron radiation source was employed whereas the sample was exposed to an ultra-high vacuum (p~10^{-9} mbar) in a flow-type He cryostat (see Ref. 12 for details). All spectra were corrected to instrumental response.

The Raman spectra were recorded by using a Renishaw inVia micro-Raman spectrometer (spectral resolution 1.5 cm^{-1}). The 514 nm line of an argon-ion laser was used for excitation. Emission was collected from the defocused laser spot of ~10 μm in diameter (to avoid photoinduced changes in the material) using a 50x objective. Silicon reference sample was used for calibration of Raman shift.

SEM micrographs were acquired with a Tescan VEGA II SBU electron microscope with an accelerating voltage of 10 kV. Energy-dispersive X-ray (EDX) spectra were recorded by Helios NanoLab 600 electron-ion dual beam microscope equipped with an EDS detector (50mm² X-Max SDD detector, Oxford Instruments). The electron beam parameters were 10 kV and 0.69 nA. The spatial stability of the beam was better than 5 nm during the measurements. The spectra were analyzed using standard procedures provided by INCA software (Oxford Instruments). As the samples were noticeably inhomogeneous, no special effort was made for calibrating the EDS detector. The estimated accuracy of quantitative results of the element analysis is better that 2%.

3. Results and discussion

The crystal structure and phase content of the samples were evaluated by Raman spectroscopy (Figs. 1 and 2). For all samples, the well-known Raman-active vibrations E_g, A_{1g} and B_{2g} of SnO_2 (cassiterite) are easily identified at 475, 634 and 775 cm^{-1}, respectively. The peaks become increasingly pronounced with increasing annealing temperature indicating marked improvement of crystalline quality. After annealing at 1400°C additional peaks at 303, 398 and 499 cm^{-1} emerge matching the Raman pattern of pyrochlore $Eu_2Sn_2O_7$. This is unsurprising as the solubility of Eu in stannia is reported to be less than 0.1% [16]. A very weak feature at 337 cm^{-1} may indicate traces of Eu_2O_3. The occurrence of this impurity phase in SnO_2:Eu has been reported in literature based on XRD analysis [7] while the Raman-pattern seems to be less sensitive to its content.

A small peak at 123 cm^{-1} (in samples without Sb) may arguably belong to the B_{1g} vibration as suggested by Ref. [13] although some sources report its position at around 100 cm^{-1} [1]. This weak Raman peak is seldom observed. Interestingly, the peak becomes exceptionally strong in Sb-doped samples and improves in proportion to Sb concentration (Fig. 2). Moreover, in Sb-doped samples additional peaks emerge at 243, 285 and ~605 cm^{-1}. The intensities of the peaks appear to be relatively insensitive to Sb concentration, yet they are completely missing in samples without Sb dopant. The peaks can not be assigned to any well-known phase of antimony oxide. Instead, they fit very closely the frequencies of the three E_u (TO) vibrational modes of SnO_2 which are normally IR-active [1]. To the best of our knowledge, no such features in the Raman spectrum of SnO_2:Sb has

been reported previously. The emergence of these bands has been noticed only for very small nanocrystallites of SnO_2 and attributed to disorder or size effect [17–19]. It is usually also reported that these features disappear after annealing at high temperatures (due to significant increase of crystallite size). In the present case, however, the heat treatment even slightly improved the visibility of the peaks (not shown) indicating that the vibrations must be due to the bulk of the lattice. Figure 3 compares the Raman spectra of SnO_2 powders containing different additives after annealing at 1400°C. It is evident that these amplified peaks are solely due to the Sb dopant and not the combined effect of Sb and Eu (unless some unintentional impurities have been incorporated during the Sb-doping). We suspect that the effect is due to a shifting of the Raman selection rule for the particular phonon mode by the structural disorder or breaking of inversion symmetry induced by the impurity [20,21] but the detailed modeling is left for future work.

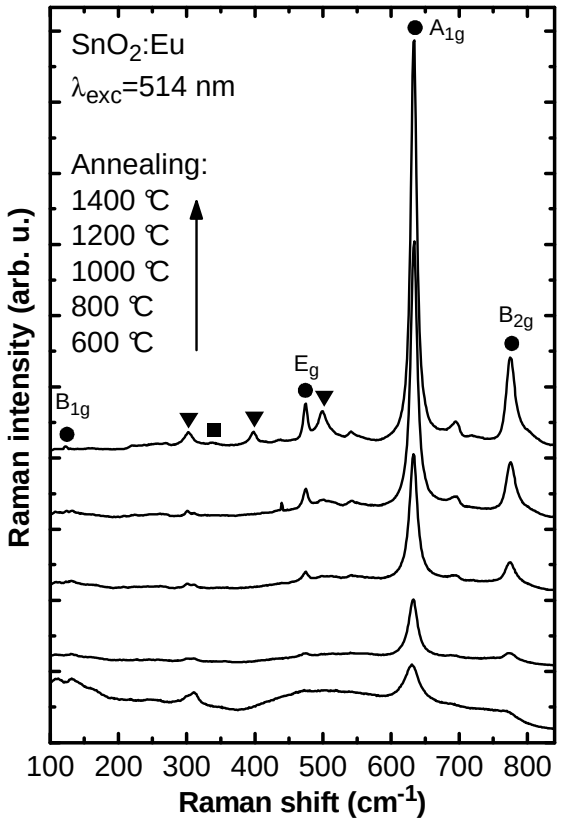

Figure 1. Raman spectra of SnO_2:Eu annealed at different temperatures. The circles (●) mark the Raman peaks of SnO_2 while the triangles (▼) indicate the peaks due to $Eu_2Sn_2O_7$ (assigned according to Refs. [13] and [14]). The rectangle (■) marks a possible peak due to cubic Eu_2O_3 [15].

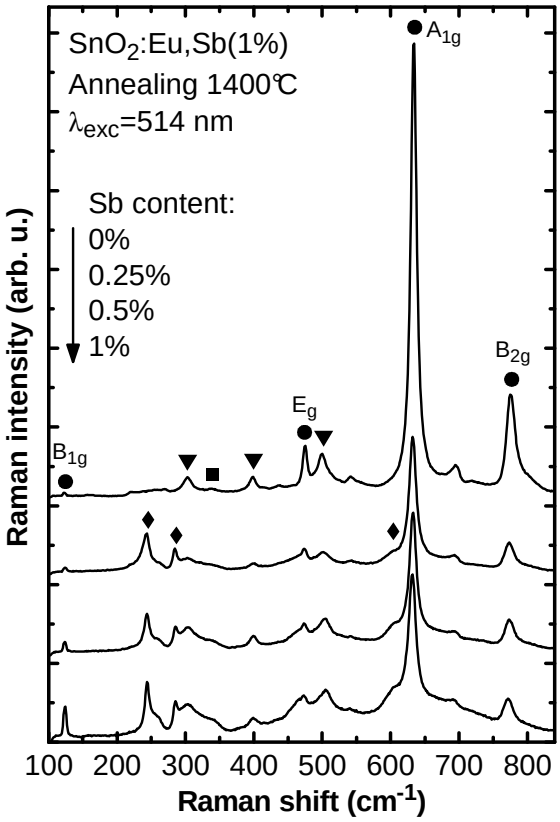

Figure 2. Raman spectra of SnO_2:Eu,Sb annealed at 1400°C in dependence on Sb concentration. Diamonds (♦) indicate peaks tentatively attributed to E_u (TO) mode of SnO_2 (other marks are the same as in Fig. 1).

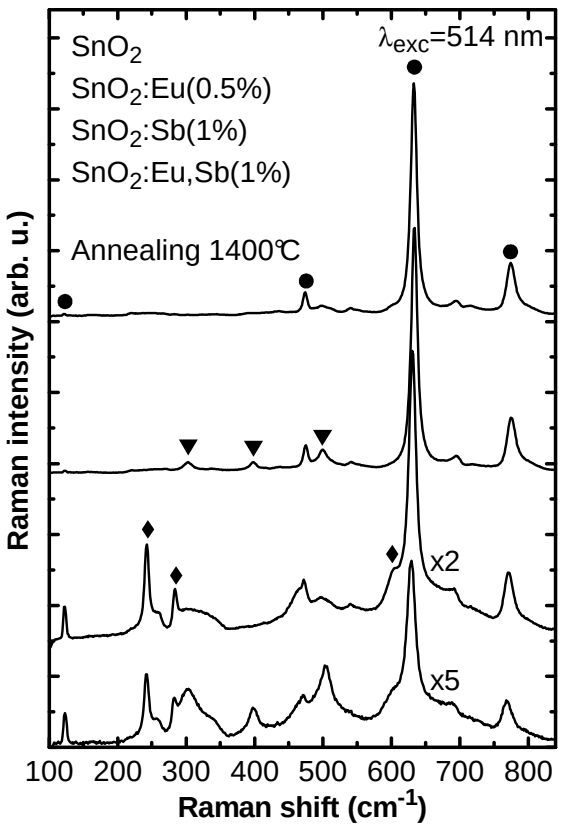

Figure 3. Comparison of the Raman spectra of SnO_2 powders with different additives annealed at 1400°C. The marking of Raman peaks is the same as in Figs. 1 and 2).

SEM micrographs indicate development of a nanostructure due to sintering (Fig. 4). A dense substance with a fairly smooth surface and no resolved granularity is observed after annealing at 600°C. Since the Raman spectrum at this annealing already indicates peaks due to stannia, the substance apparently consists of fine crystallites embedded into amorphous medium. Higher annealing temperatures induce initially a porous structure in the material until a granular morphology is formed after annealing at 1200°C. Finally, after annealing at 1400°C, a coarse nanoparticulate material with characteristic particle size about 200–300 nm is achieved. However, rather peculiar structure development was observed for samples co-doped with antimony and annealed at 1400°C. In this case a material consisting of single crystals (up to tens of microns in size) mixed with smaller pieces of "debris" was obtained (Fig. 5a). Moreover, EDX analysis of the large crystals and the fine-grained substance indicates that the latter contains much higher concentration of Eu (Fig. 5b,c). This suggests that the antimony-induced enhanced growth of crystallites rejects the Eu dopant, probably due to the small solubility of Eu in bulk stannia.

The annealing temperature 1400°C is already quite close to the melting point for pure stannia, 1630°C [22]. It is well-known that impurities reduce the melting point of pure substance which may provide a trivial explanation for the enhanced growth of crystallites in Sb-doped samples.

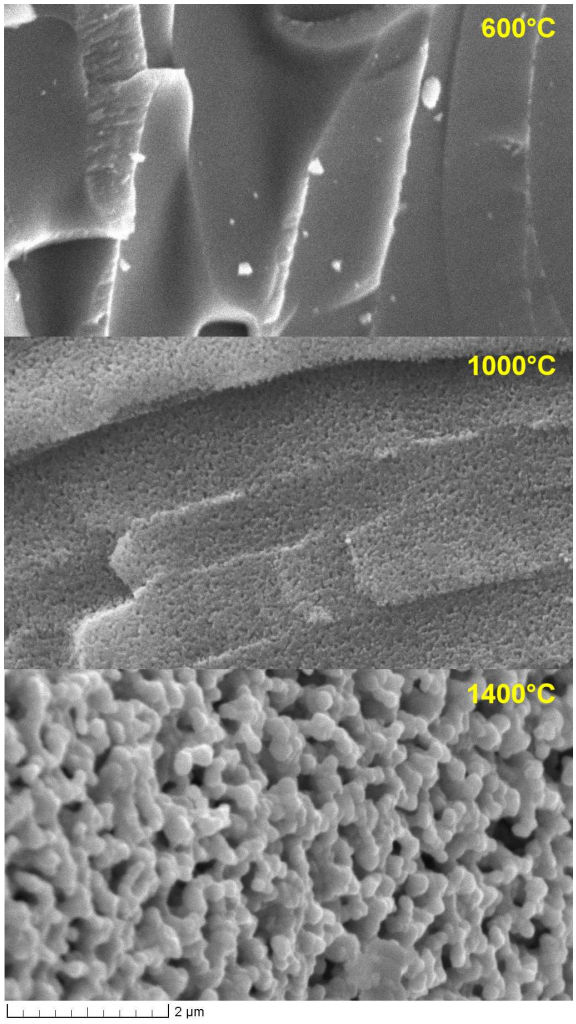

Figure 4. SEM micrographs of SnO_2:Eu powders annealed at 600, 1000 and 1400°C.

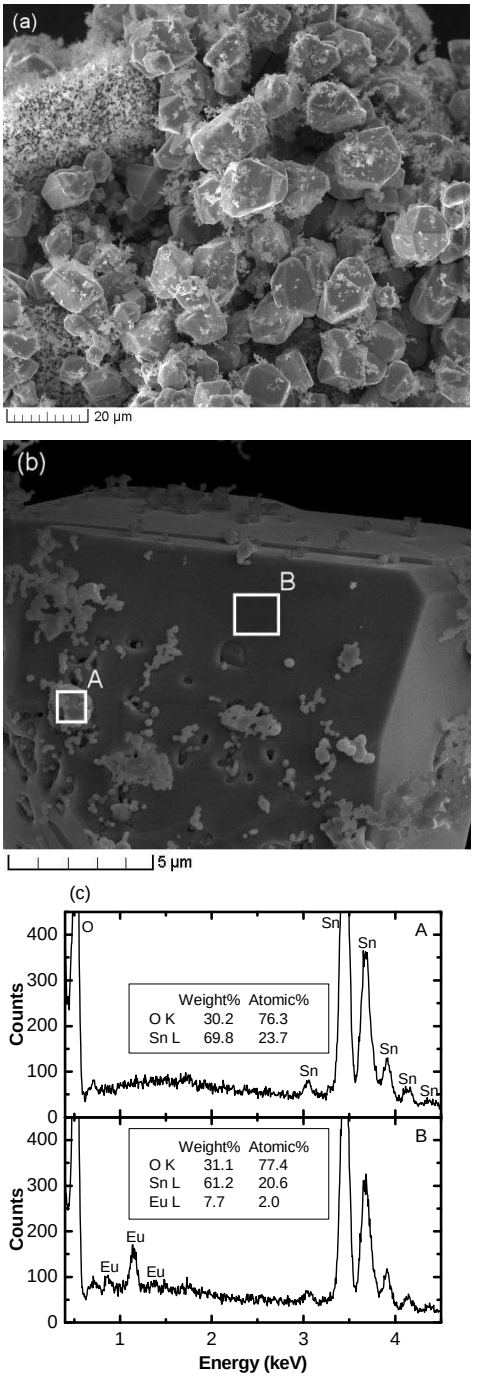

Figure 5. (a) SEM micrograph of SnO_2:Eu,Sb (0.5%) powder annealed at 1400°C; (b) zoomed-in to one crystal; (c) EDX spectra corresponding to the two marked areas.

Excitation of the material with 464 nm radiation (i.e. direct excitation in resonance with the Eu^{3+} 4f transition $^7F_0 \rightarrow {}^5D_2$) leads generally to an emission spectrum containing a mixture of sharp lines and broad bands (Fig. 6). Up to 1200°C, the broad bands are prevailing (especially the $^5D_0 \rightarrow {}^7F_2$ electric dipole transition), so we can conclude that the Eu^{3+} ions are mainly situated in disordered surrounding. However, after annealing at 1400°C the broadband emission is suppressed and the strength of sharp emission lines (mainly the $^5D_0 \rightarrow {}^7F_1$ magnetic dipole transition) is drastically increased which suggests that nearly all Eu ions that were previously located in disordered surrounding became incorporated into regular lattice sites. These observations suggest that up to 1200°C of thermal treatment, marked amount of amorphous media and other disordered sites (e.g. crystallite surfaces) are available for the RE impurities. The prevailing of the $^5D_0 \rightarrow {}^7F_1$

magnetic dipole transition in crystalline sites suggests that Eu^{3+} substitutes Sn^{4+} in a regular lattice site which has center symmetry (symmetry group D_{2h}).

In contrast, under 266 nm excitation all samples exhibited only sharp PL lines typical of Eu^{3+} in crystalline SnO_2 surrounding (Fig. 7). The result is natural since 266 nm radiation is supposed to be absorbed by SnO_2 host and Eu ions become excited through an energy transfer. The emission intensity has a very steep dependence on heat treatment increasing more that 4 orders of magnitude as the sintering temperature varies from 600°C to 1400°C. This is in accordance with the results of direct excitation which indicate that marked amount of Eu becomes incorporated into crystalline phase only after annealing at 1400°C. Annealing at 1400°C seems still not fully optimizing the host-sensitized Eu emission (see inset of Fig. 7). Comparison to commercially available highly efficient phosphors operating within this spectral range reveals a rough estimate of 5% for the overall quantum yield.

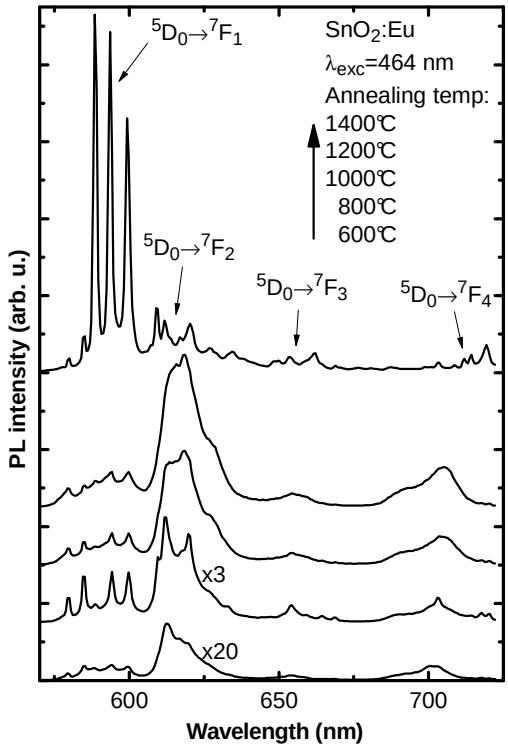

Figure 6. PL spectra of SnO_2:Eu annealed at different temperatures under 464 nm excitation.

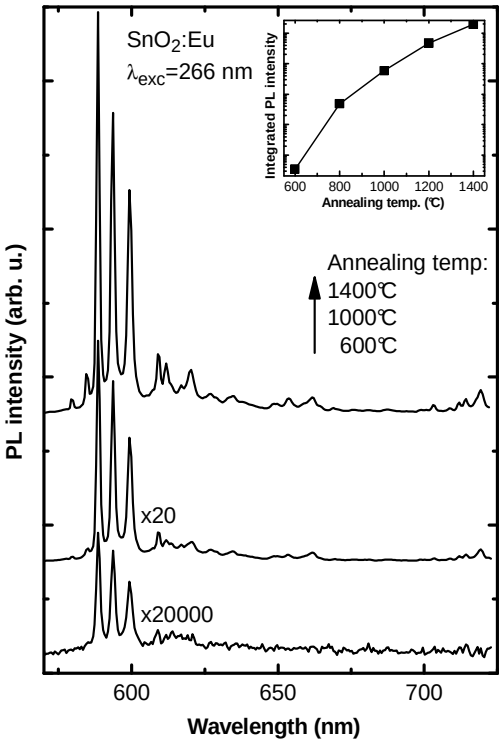

Figure 7. PL spectra of SnO_2:Eu annealed at different temperatures under 266 nm excitation. The inset depicts the integrated PL intensity (in log-scale) on annealing temperature.

In order to gain further insight on the possible reasons limiting the luminescence efficiency of SnO_2:Eu under host-mediated excitation, PL decay curves as well as temperature-dependence of PL excitation spectra were recorded. The PL decay curves (Fig. 8) can be considered as containing roughly two regimes. The initial fast decay characterizes the ions situated close to crystallite surface (but still in regular sites according to spectral fine structure) and experiencing non-radiative decay due to quenching centers (e.g. OH-groups, which are known as efficient quenchers of RE emission). The following longer decay can be roughly approximated with a single exponential function with a decay time of 15–20 ms (a fitting example is shown). The latter is in correspondence to the rate of the prevalent $^5D_0 \rightarrow ^7F_1$ magnetic dipole transition (~50 s^{-1} according to Ref. 23) which is known to be nearly independent of the surrounding (i.e. the symmetry of the emission center). No marked temporal stretching of the emission due to hindered energy transfer from host to guest is evident in the case of this host, in contrast to TiO_2 [3]. Moreover, the decay time of the long decay component does not appreciably depend on annealing treatment suggesting that the quenching of Eu^{3+} emission does not take place evenly across the bulk of the crystal but is confined to a particular fraction of

emission centers (e.g. those located near crystallite surface or other regions close to quenching centers). The contribution of the fast decay, however, is systematically reduced with the increasing annealing temperature (due to the decreasing role of quenching centers) until it nearly disappears after annealing at 1400°C.

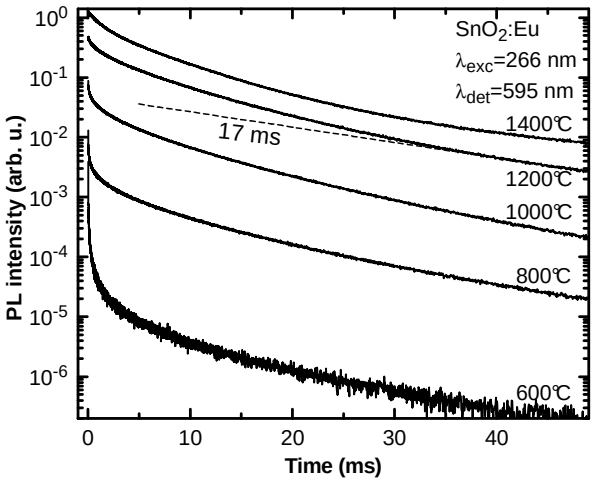

Figure 8. Host-sensitized PL decay kinetics of SnO_2:Eu in dependence on annealing temperature.

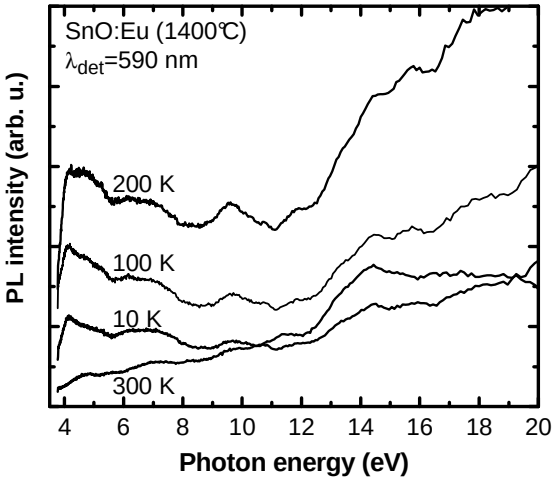

Figure 9. Excitation spectrum of SnO_2:Eu^{3+} annealed at 1400°C.

The excitation spectrum of the Eu^{3+} emission (Fig. 9) reveals a rather extended excitation band starting roughly at 350 nm or 3.6 eV which is correlating fairly well with the absorption edge of SnO_2 [24]. The excitation spectrum extends far into the VUV range and spans the theoretically modeled band-to-band absorption spectrum of SnO_2 [25]. All these observations imply that the excitation of Eu^{3+} is achieved through an energy transfer from the host. However, it is noteworthy that in contrast to the results depicted in Fig. 9, a number of previous works on SnO_2:Eu report a much more localized excitation band around 300 nm [7,10] which may indicate significant contribution of charge transfer excitation in those cases.

Interestingly enough, the PL intensity has a rather peculiar dependence on temperature achieving maximum at around 200 K and rapidly decreasing at higher temperatures. While the increasing part of the dependence may be possible to explain by thermally induced energy level population dynamics, some thermally activated quenching mechanism must account for the decreasing part. Slightly less-pronounced quenching of Eu^{3+} emission has been previously reported by Morais et al. [8] who has compared 0.1 and 0.5 at% Eu-doped samples and achieved stronger quenching with higher doping. Therefore the quenching might be connected to energy migration among Eu^{3+} ions and energy transfer to quenching centers, especially surface defects in nanophase [26]. Multiphonon relaxation mechanism is improbable for Eu^{3+} at these temperatures as also suggested by the behavior of the PL decay curves (Fig. 8).

As mentioned previously, the quantum efficiency of the host-sensitized Eu^{3+} emission at room temperature is roughly 5%. This would place the efficiency of the emission at 200 K to an adequate level of ~50% which is, moreover, nearly constant over the 100–300 nm spectral range of excitation and therefore promising for a number of applications if it will be possible to suppress the quenching mechanism by suitable preparation of material.

Finally, the influence of antimony co-dopant on PL properties of Eu^{3+} was studied. It appears that incorporation of Sb severely affects Eu emission intensity (Fig. 10) which is reduced nearly exponentially with increasing Sb concentration. Correspondingly, the PL decay kinetics (Fig. 11) indicates increasingly pronounced contribution of the fast decay component as the concentration of Sb is increased. The lifetime of the longer decay component remains almost unchanged. The heat treatment of Sb-doped samples improved the emission intensity up to 1200°C whereas annealing at 1400°C markedly quenched the emission (not shown). This appears to correlate with the formation of the large microcrystals in Sb-doped samples as observed in SEM micrographs (Fig. 5). In

summary, all these observations suggest that the quenching effect is unlikely to be due to an energy transfer to Sb-induced defect levels or free carriers. Instead, it seems that lesser amount of Eu becomes incorporated in the crystallites as Sb concentration is increased. This conclusion is also suggested by EDX analysis (Fig. 5c).

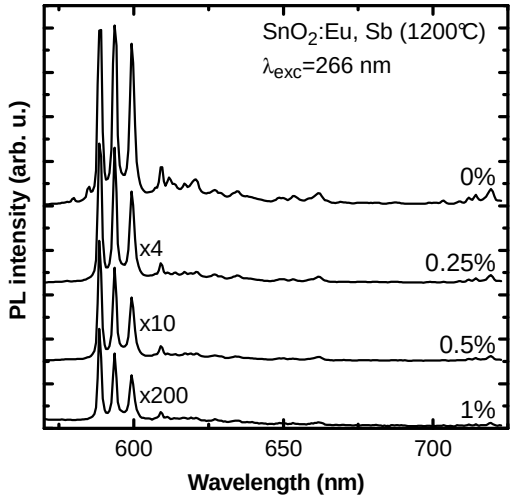

Figure 10. Host-sensitized PL spectra of SnO_2:Eu,Sb annealed at 1200°C in dependence on Sb concentration.

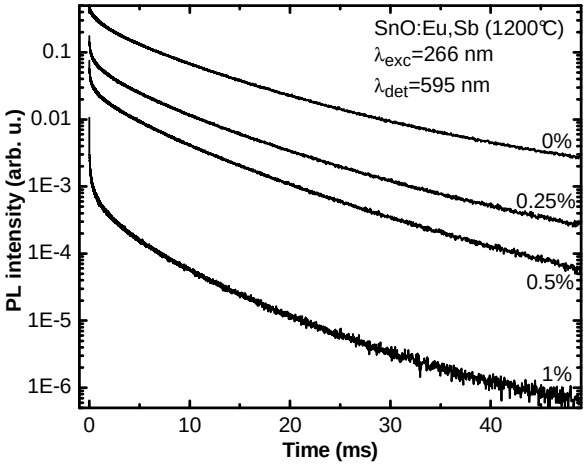

Figure 11. Host-sensitized PL decay kinetics of SnO_2:Eu,Sb (annealed at 1200°C) in dependence on Sb concentration.

4. Conclusions

It is concluded that europium-doped stannia obtained by a sol-gel route requires thermal treatment temperatures exceeding 1400°C in order to optimize host-sensitized emission intensity of the rare earth activator. In particular, thermal treatment at 1400°C finally leads to the disappearance of Eu^{3+} centers in disordered surrounding. While Sb co-dopant immensely improves crystallization at 1400°C, the process also stimulates segregation Eu dopants and corresponding quenching of Eu^{3+} emission. Host-sensitized Eu emission has considerable intensity at ~200 K being partially quenched at room temperature. The effect may be due to the presence of quenching centers in nanocrystalline material.

An interesting finding is that Sb-doping in SnO_2 results in a rather pronounced amplification of a weak Raman band at 123 cm^{-1} and activation of certain IR frequencies in the Raman spectrum.

Acknowledgements

Estonian Science Foundation is acknowledged for financial support (grants nos. 7456 and 7612). Microscopy and microanalysis is partially supported by Estonian Nanotechnology Competence Centre (EAS grant no EU 29996). Financial support for synchrotron experiments was provided within EU grant II-20060076 EC. The authors are grateful to Ilmar Kink for EDX analysis and Chong-Geng Ma for fruitful discussion.

References

[1] M. Batzill and U. Diebold, Progress in Surface Science 79 (2005) 47.
[2] U. Diebold, Surf. Sci. Reports 48 (2003), 53.
[3] V. Kiisk, V. Reedo, O. Sild, and I. Sildos, Optical Mat. 31 (2009) 1376.
[4] S.N.B. Bhaktha, et al., Appl. Phys. Lett. 93 (2008) 211904.
[5] P. Psuja, D. Hreniak, and W. Strek, J. Nanomat. vol. 2007, article ID 81350.
[6] Y. Li and R. Almeida, Appl. Phys. B 98 (2010) 809.
[7] S.S. Chang and M.S. Jo, Ceram. Int. 33 (2007) 511.
[8] E. Morais, L. Scalvi, A. Tabata, J. De Oliveira, and S. Ribeiro, J. Mater. Sci. 43 (2008) 345.
[9] X. Fu, H. Zhang, S. Niu, and Q. Xin, J. Solid State Chem. 178 (2005) 603.

[10] C.-T. Lee, F.-S. Chen, and C.-H. Lu, J. Alloys & Comp. 490 (2010) 407.
[11] V. Kessler, J. Sol-Gel Sci. Tech. 51 (2009) 264.
[12] M. Kirm, J. Aarik, M. Jürgens, and I. Sildos, Nucl. Instr. Meth. A. 537 (2005) 251.
[13] P.S. Peercy and B. Morosin, Phys. Rev. B 7 (1973) 2779.
[14] T.T. Zhang, K.W. Li, J. Zeng, Y.L. Wang, X.M. Song, and H. Wang, J. Phys. Chem. Solids 69 (2008) 2845.
[15] L.A. Tucker, F.J. Carney, P. McMillan, S.H. Lin, and L. Eyring, Appl. Spectrosc. 38 (1984) 857.
[16] T. Matsuoka, T. Tohda and T. Nitta, J. Electrochem. Soc. 130 (1983) 417.
[17] F.H. Aragón, J.A.H. Coaquira, P. Hidalgo, S.W. da Silva, S.L.M. Brito, D. Gouvêa, and P.C. Morais, J. Raman Spectr. (2010), in press.
[18] M.N. Rumyantseva, A.M. Gaskov, N. Rosman, T. Pagnier, and J.R. Morante, Chem. Mater. 17 (2005) 893.
[19] J. Beltran, L. Sánchez, J. Osorio, L. Tirado, E. Baggio-Saitovitch, and C. Barrero, J. Mat. Sci. 45 (2010) 5002.
[20] T. Kamijoh, A. Hashimoto, N. Watanabe, and M. Sakuta, Phys. Rev. B 33 (1986) 7281.
[21] R.T. Harley, J.B. Page Jr., and C.T. Walker, Phys. Rev. B 3 (1971) 1365.
[22] CRC Handbook of Chemistry and Physics, 88th edition.
[23] R. Reisfeld, E. Zigansky and M. Gaft, Molecular Physics 102 (2004) 1319.
[24] V.T. Agekyan, phys. stat. sol. (a) 43 (1977) 11.
[25] Z.Q. Li, Y.L. Yin, X.D. Liu, L.Y. Li, H. Liu, and Q.G. Song, J. Appl. Phys. 106 (2009) 083701.
[26] J. Wang, H. Song, X. Kong, W. Xu, J. Appl. Phys. 91 (2002) 9466.